Facilitated Detection and Quantification of Theragnostic Magnetocapsules by Analyzing MRI Susceptibility Perturbations

P. H. Mills[1,2], T. Link[3], A. Arepally[3], J. D. Thompson[4], J. W. Bulte[3], and E. T. Ahrens[1,2]

[1]Department of Biological Sciences, Carnegie Mellon University, Pittsburgh, PA, United States, [2]Pittsburgh NMR Center for Biomedical Research, Pittsburgh, PA, United States, [3]Institute for Cell Engineering, Johns Hopkins School of Medicine, Baltimore, MD, United States, [4]Division of Materials Science & Technology, Group 10, Los Alamos National Laboratory, Los Alamos, NM, United States

Introduction Recently, non-invasive imaging studies have been used to follow the delivery and engraftment of pancreatic islets that are encapsulated in shells composed of alginate crosslinked with poly-L-lysine and containing the FDA-approved superparamagnetic iron-oxide (SPIO) Feridex (Berlex Labs, Montville NJ) (1). These capsules are stable, have a uniform diameter, and contain a Feridex iron content that is three orders of magnitude higher than typical SPIO-labeled cells. Each capsule is permeable to metabolites, but not native antibodies, thus immunosuppressive therapy is reduced or completely avoided. These capsules facilitate MRI-tracking of grafted islets while offering immunoprotection.

Detecting SPIO deposits in conventional MRI presents a challenge when contrast is subtle relative to intrinsic sources. Here, we apply a post-processing method, called Phase map cross-correlation Detection and Quantification (PDQ) (2), that can automatically identify magnetocapsules throughout an MRI volume, count them, and measure their magnetic moment. The PDQ method has previously been shown to generate stark positive-contrast images, provides quantitative analysis of label cell numbers, and works effectively even in low-SNR images (2).

We apply the PDQ method to a gel phantom containing ~10^3, 450 µm diameter magnetocapsules. The magnetocapsules were made with three different Feridex concentrations (10%, 5%, and 2.5% v/v). Using standard volumetric MRI data, apparent magnetocapsules were automatically detected, counted, and the magnetic moment per capsule was calculated. For verification, the average magnetic moment of the 10% Feridex magnetocapsules was measured using a SQUID magnetometer.

Theory An MRI dataset is generally complex-valued, and typically only the magnitude image is displayed while phase angle information is discarded. A voxel's phase angle is proportional to its local magnetic field as:

$$\phi = \gamma \cdot TE \cdot \Delta B_Z \qquad [1]$$

where γ is the gyromagnetic ratio, *TE* is echo time, and ΔB_z is the difference in magnetic field strength relative to the primary magnetic field, B_0. We assume each magnetocapsule is a spherical SPIO deposit, and that it behaves as a magnetic dipole, creating a magnetic field perturbation that can be described analytically by (3):

$$\Delta B_Z(r,\theta) = \frac{\Delta\chi B_0}{3}\left(\frac{a}{r}\right)^3 (3\cos^2\theta - 1) \qquad [2]$$

where $\Delta\chi$ is the magnetic susceptibility difference between the spheroid and background material, *a* is spheroid radius, *r* is distance from its center, and θ is the angular deviation from the direction of B_0. The PDQ method combines Eqs. [1]& [2] to generate a 3D phase-offset 'dipole template,' then calculates the normalized cross-correlation value between the template and high-resolution MRI phase data to identify occurrences of a magnetic dipole (4). Cross-correlation overlays the search template onto every template-sized patch in the phase image, resulting in a 3D similarity matrix image that contains positive-contrast spots indicating apparent dipoles (i.e., magnetocapsules) against a null background. As dipoles are located throughout a volume, their biodistribution can be visualized and their magnetic moment measured. To measure the magnetic moment of each SPIO deposit, a Least-Squares Fit (LSF) can be made between its phase-image impression and the template. Assuming magnetocapsules have the same radius, the resulting LSF fit value for each magnetocapsule can be combined with Eqs. [1] & [2] to back-calculate $\Delta\chi$ for a particular deposit. The susceptibility can then be used to calculate the magnetic moment of the SPIO deposit using the relation:

$$m\ (\text{emu}) = 1000\frac{4\pi a^3 B_0}{3\mu_0} \Big/ \left(\frac{1}{\chi} + 1\right) \qquad [3]$$

where μ_0 = 1.26e-6 T·m/A is the permeability of free space.

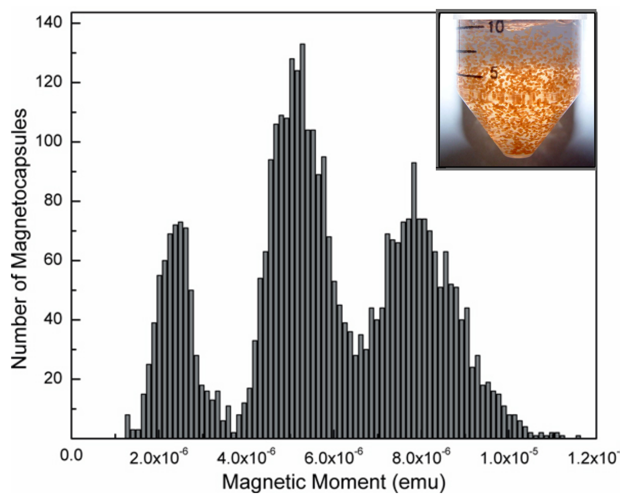

FIG. 1. PDQ-calculated magnetic moment distribution for 3,692 individual magnetocapsules. Magnetocapsules were randomly dispersed in 12 separate agarose gel phantoms. Numerical magnetic moment values are in Table 1. PDQ's ability to measure magnetic moment is demonstrated by its strong correlation to Feridex concentration. This distribution also suggests that PDQ results are sufficiently consistent across separate MRI scans to allow for compiling and comparing results between different samples. Inlay shows typical sample consisting of 1000+ capsules suspended in agarose gel.

Methods MRI data were acquired at 4.7 T using a 3D gradient-echo (GRE) pulse sequence on a set of 12 agarose gel phantoms containing 2.5%, 5%, and 10% (v/v) Feridex magnetocapsules in suspension (n=3, 5, 4 respectively). Imaging parameters were TE/TR=1.2/300 ms, 133 µm isotropic resolution, and 18 signal averages. Resulting MR phase data were unwrapped using Prelude, a 3D unwrapping algorithm (5). Background magnetic field phase-encoding ramps were removed by fitting and subtracting a linear gradient from each volumetric dataset. 3D templates sized 9×9×9 pixels (1197 µm) were generated from Eqs. [1] & [2], and cross-correlation was applied. The resulting similarity matrix image was thresholded so that all dipoles with a value in the range [0.3, 1.0] were considered. The magnetic moment for each dipole was calculated using Eq. [3]. To validate the PDQ measurements, the magnetic moments for 100 and 200 magnetocapsules (10% v/v Feridex) were measured using a commercial SQUID magnetometer at 310 K between 1 to 7 T and normalized to a single capsule.

TABLE 1. Properties of each type of magnetocapsule. The measurement denoted 'SQUID' was found using a magnetometer, measurements denoted 'PDQ' resulted from PDQ analysis, and those denoted 'estimate' were calculated by extending the SQUID measurement to the 5% and 2.5% Feridex magnetocapsules.

Magnetocapsule (v/v)	Diameter (microns)	Magnetic Moment (emu) (B_0=4.7 T, 310 K)	Magnetic Moment (emu) (PDQ Measurement)	Difference in Magnetic Moment	Volume Susceptibility (dimensionless) (estimate)
10% Feridex	450 +/- 40	8.1 +/- 0.2 e-6 (SQUID)	8.0 +/- 0.8 e-6 (PDQ)	1%	1.9 e-5
5% Feridex	450 +/- 40	4.1 +/- 0.2 e-6 (estimate)	5.2 +/- 0.6 e-6 (PDQ)	21%	0.96 e-5
2.5% Feridex	450 +/- 40	2.0 +/- 0.2 e-6 (estimate)	2.4 +/- 0.4 e-6 (PDQ)	17%	0.48 e-5

Results / Conclusions Fig. 1 displays PDQ's magnetic moment measure for 3,692 magnetocapsules of different Feridex concentrations. The correlation between Feridex concentration and magnetic moment is consistent across multiple samples and MRI scans. Table 1 shows the properties of each magnetocapsule type, and compares PDQ's magnetic moment measurement to that directly measured by SQUID. MRI-based PDQ reported magnetic moments within 1-21% of the SQUID-measured values. In general, since the magnetic moment of these magnetocapsules is known beforehand, the PDQ method can search throughout a tissue volume for each occurrence of a therapeutic magnetocapsule. Importantly, the PDQ method requires no special pulse sequences and works on previously-acquired data. Automatic analysis and capsule counting using the PDQ method may find applications in islet/magnetocapsule transplantation studies using a large animal model, such as diabetic swine, where ≥100,000 capsules are injected and where the capsule integrity (intact vs. ruptured) is an important predictor of islet immunoprotection and survival.

References
1. Barnett B.P. et al., *Nat Med 2007*; 13:986-991
2. Mills P.H. et al., *Magn Reson Imaging* 2008; 26:618-628
3. Schenck J.F., *Med Phys* 1996; 23:815-850
4. Lewis J.P., *Vis Interface* 1995:120-123
5. Jenkinson M., *Magn Reson Med* 1993; 49:193-197